**Original citation:**
Zhang, Junliang, Tanaka, Joji, Gurnani, Pratik, Wilson, Paul, Hartlieb, Matthias and Perrier, Sébastien. (2017) Self-assembly and dis-assembly of stimuli responsive tadpole-like single chain nanoparticles using a switchable hydrophilic/hydrophobic boronic acid cross-linker. Polymer Chemistry, 28 (8). pp. 4079-4087.

**Permanent WRAP URL:**
http://wrap.warwick.ac.uk/93551

**A note on versions:**
The version presented here may differ from the published version or, version of record, if you wish to cite this item you are advised to consult the publisher's version. Please see the 'permanent WRAP URL' above for details on accessing the published version and note that access may require a subscription.

For more information, please contact the WRAP Team at: wrap@warwick.ac.uk

# Journal Name

## ARTICLE

# Self-assembly and dis-assembly of stimuli responsive tadpole-like single chain nanoparticles using a switchable hydrophilic/hydrophobic boronic acid cross-linker

Junliang Zhang,[a] Joji Tanaka,[a] Pratik Gurnani,[a] Paul Wilson,[a] Matthias Hartlieb[a] and Sébastien Perrier*[a,b,c]

Living systems are driven by molecular machines that are composed of folded polypeptide chains, which are assembled together to form a multimeric complex. Although replicating this type of systems is a long standing goal in polymer science, the complexity of the structures imposes is synthetically very challenging, and generating synthetic polymers to mimic the process of these assemblies appears to be a more appealing approach. To this end, we report a linear polymer programmable for stepwise folding and assembly to higher-order structures. To achieve this, a diblock copolymer composed of 4-Acryloylmorpholine and glycerol acrylate was synthesised with high precision *via* reversible addition fragmentation chain transfer polymerisation ($Đ < 1.22$). Both intramolecular folding and intermolecular assembly was driven by pH responsive cross-linker, benzene-1,4-diboronic acid. The resulting intramolecular folded single chain nanoparticles were well defined ($Đ < 1.16$) and successfully assembled into a multimeric structure ($D_h = 245$ nm) at neutral pH with no chain entanglement. The assembled multimer was observed with a spherical morphology as confirmed by TEM and AFM. These structures were capable of unfolding and disassembling either at low pH or in the presence of sugar. This work offers new perspective for the generation of adaptive smart materials.

## Introduction

Nature uses the sophisticated machinery of the cell to confer precision on its biopolymers (e.g. proteins) in one-dimension through their primary sequences, and in three-dimensions (3D) via their subsequent secondary and tertiary structures, as well as their molecular organisation into multimeric complexes, all of which are imperative for the polymers to perform their specific biological functions. The 3D architectures of proteins originate from the controlled dynamic folding process of a single-stranded polypeptide chain and further self-assembling into selectively tailored molecular assemblies and interfaces which interact and respond to their environment.[1-4] Folding a single linear polymer chain into a single chain nanoparticle (SCNP) has been utilized as a versatile way of constructing polymeric nanoparticles to copy nature's ability to form well-defined structures and is a rapidly expanding research area in polymer science.[5-30] SCNPs can not only mimic the delicate controlled folding process of proteins with controlled size and morphology,[31-33] but can also self-assemble into more complexed 3D structures.[34] Furthermore stimuli-responsive polymeric nanoparticles, also called "smart" or "intelligent" nanoparticles that

are capable of conformational and chemical changes by adapting the external stimuli[35, 36] have increasingly attracted interest due to their diverse range of applications in delivery and release of drugs,[37, 38] diagnostics,[39] sensors.[40] Dynamic covalent chemistry is a very suitable candidate for building intelligent materials which can be responsive to the environmental changes, such as pH or input stimuli.[33, 41-44] Boronic acid containing macromolecules have been widely utilized as an effective route toward bioresponsive architectures and a large body of research has been carried out.[45-51] Boronic acid derivatives reversibly react with 1,2- and 1,3-diols (*i.e.* saccharides) to form boronic or boronate ester depending on the environmental pH.[52] At high pH, the anionic boronate ester is hydrophilic (Scheme 1a). Upon acidification the boronate moieties will be converted to neutral/hydrophobic groups (Scheme 1b).[53, 54] Sumerlin *et al.* reported a novel example of boronic acid containing triply-responsive "schizophrenic" diblock copolymers which displayed self-assembly in response to changes in temperature, pH, and the concentration of diol.[52]

The self-assembly of amphiphilic diblock copolymers have attracted considerable interest to generate stimuli responsive nanoparticles with tailored structures.[35, 55-57] The structures and properties of superparticles formed by self-assembled SCNPs have been proved to be entirely different from traditional block copolymer micelles.[58] Zhao *et al.*[59] and Chen *et al.*[58] reported the first examples of self-assembly and disassembly of diblock single chain Janus nanoparticles (SCJNPs). However, these self-assemblies were obtained either in organic solvent or requiring the involvement of organic solvent to assist the solubility of the hydrophobic part, which will limit the application in physiological conditions. Besides, the disassembly was achieved

[a.] Department of Chemistry, The University of Warwick, Coventry CV4 7AL, U.K.
[b.] Warwick Medical School, The University of Warwick, Coventry CV4 7AL, U.K.
[c.] Faculty of Pharmacy and Pharmaceutical Sciences, Monash University, 381 Royal Parade, Parkville, Victoria 3052, Australia. Email: s.perrier@warwick.ac.uk; Tel: +44 2476 528 085
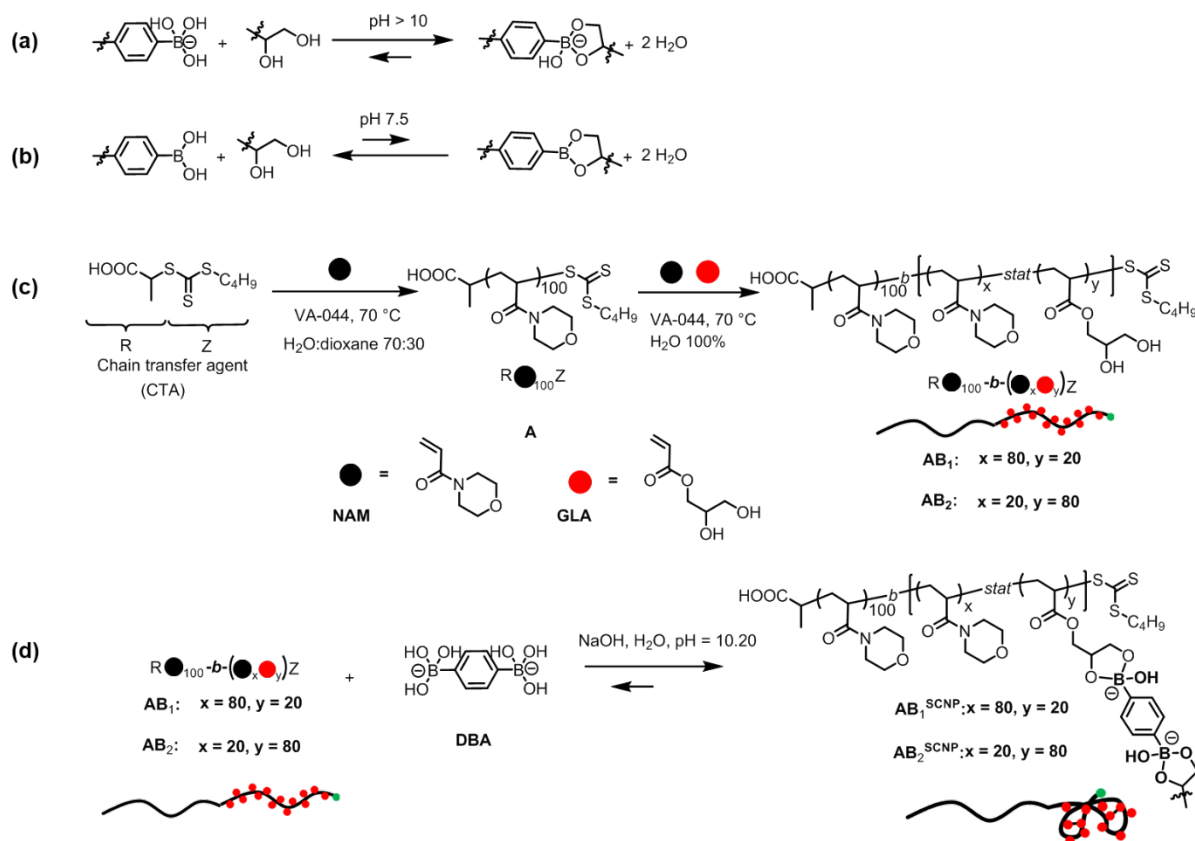
**Scheme 1**. **a)** Equilibrium formation of boronate esters from 1,2-diols at high pH in water; **b)** Equilibrium formation of boronic esters from 1,2-diols at neutral pH in water; **c)** Schematic representation of the synthesis of hydrophilic diblock copolymers of **AB₁** and **AB₂** by RAFT polymerization. **d)** Schematic representation of the synthesis of tadpole-like SCNPs.

by utilizing the ultra-sonication which will also circumvent its wide use due to the destructive effect of sonication.[60]

Herein, we report a novel synthesis of completely water soluble SCNPs from a 1,2-diol pendant linear precursor polymer, using a boronic acid cross linker and utilising the aforementioned pH dependency of boronate esters to promote self-assembly. In contrast to the studies of Zhao *et al.* and Chen *et al.*, we investigated self-assembly without the need for switching solvents and also new to this field we investigated the dis-assembly of the SCNPs back to the linear precursor using pH and sugars as chemical stimuli.

## Results and discussion

In the present contribution, 4-Acryloylmorpholine (NAM) and glycerol acrylate (GLA, synthesized by adapting to the published procedure,[61] Scheme S1, Figure S1 and S2) were used as monomers to fabricate water soluble, 1,2-diol-containing copolymers. Two diblock copolymers were designed with an initial hydrophilic block of poly(NAM) (Block **A**), comprising 100 units, to impart water solubility for the later self-assembled structure followed by a statistical hydrophilic segment of NAM/GLA (Block **B**, 100 units in total) able to react with a suitable diboronic acid cross-linker to form tadpole-like SCNPs.

In order to investigate the effect of the relative molar fractions of the hydrophobic block for self-assembly behaviour of the SCNPs, two different compositions of **B** block copolymers were

synthesized: PolyNAM₁₀₀-*b*-Poly(NAM₈₀-*stat*-GLA₂₀) (**AB₁**) and PolyNAM₁₀₀-*b*-Poly(NAM₂₀-*stat*-GLA₈₀) (**AB₂**). As illustrated in Scheme 1c, optimized RAFT conditions as previously described for the synthesis of water soluble multiblock copolymers (azoinitiator: VA-044 at 70 °C in H₂O),[62] were applied to provide a fast (within 2 hours) and quantitative monomer conversion while maintaining high control over molar mass, narrow dispersity, and high theoretical livingness. 2-[(Butylthio-carbonothioyl)thio]propanoic acid [called (propanoic acid)yl butyl trithiocarbonate (PABTC) in this paper] and 2, 2'-azobis[2-(2-imidazolin-2-yl)propane]dihydrochloride (VA-044) were used as the chain transfer agent (CTA) and the initiator respectively. After 2 h of polymerization of each block (See the Supporting Information for a detailed procedure), near quantitative monomer conversion (> 99%) was obtained and confirmed by ¹H NMR spectroscopy analysis for both diblock copolymers (Figures S3 and S4). ¹H NMR spectroscopy of both diblock copolymer confirmed the presence of the peaks associated with each segment, especially the presence of the diol functional group at 4.81 and 4.64 ppm (Figures S3 and S4, signals a and a'). Size exclusion chromatography (SEC) in DMF revealed a monomodal distribution and a shift towards higher molar mass confirming the successful chain extension after polymerization (Figures S5 and S6). While a narrow dispersity was detected for both copolymers [PNAM₁₀₀-*b*-(PNAM₈₀-GLA₂₀), **AB₁**, Đ = 1.14; PNAM₁₀₀-*b*-(PNAM₂₀-GLA₈₀), **AB₂**, Đ = 1.22, Table 1), it needs to be noted that, for the **AB₂** copolymer, a low molar mass tail was observed in the chromatogram (Figure S6).

**Table 1.** Characterization of the linear copolymers, SCNPs by ^{1}H NMR spectroscopy, DMF-SEC, DLS and DSC.

| Sample | Composition | $M_{n,th}$[a] g mol$^{-1}$ | $M_{p,SEC}$[b] g mol$^{-1}$ | $M_{n,SEC}$[b] g mol$^{-1}$ | $Đ$[b] | $<G>$[c] | $D_h$[d] nm | PDI[d] | $T_g$[e] °C |
|---|---|---|---|---|---|---|---|---|---|
| **A** | PNAM$_{100}$ | 14400 | 14800 | 14100 | 1.07 | - | - | - | 159.2 |
| **AB$_1$** | PNAM$_{100}$-$b$-P(NAM$_{80}$-$stat$-GLA$_{20}$) | 28600 | 27200 | 23700 | 1.14 | - | 7.7 | 0.07 | 147.9 |
| **AB$_1^{SCNP}$** | PNAM$_{100}$-$b$-[P(NAM$_{80}$-$stat$-GLA$_{20}$)]$^{SCNP}$ | - | 24400 | 19900 | 1.17 | 0.90 | 6.1 | 0.05 | 172.4 |
| **AB$_2$** | PNAM$_{100}$-$b$-P(NAM$_{20}$-$stat$-GLA$_{80}$) | 28900 | 27700 | 22100 | 1.22 | - | 6.5 | 0.08 | 95.8 |
| **AB$_2^{SCNP}$** | PNAM$_{100}$-$b$-[P(NAM$_{20}$-$stat$-GLA$_{80}$)]$^{SCNP}$ | - | 23700 | 20300 | 1.16 | 0.86 | 5.0 | 0.08 | 172.6 |

[a] $M_{n,th}$ = [M]$_0$ × $p$ × $M_M$/[CTA]$_0$ + $M_{CTA}$, $p$ is the monomer conversion determined by ^{1}H NMR spectroscopy.

[b] Determined by SEC in DMF with PMMA used as molecular weight standards, $M_p$ represents the maximum peak value of the size-exclusion chromatogram.

[c] Compaction parameter $<G>$ = $M_{p,SCNP}$/$M_{p,linear}$, the molecular weight variation caused by the cross-linking reaction (*e.g.* the increased DBA units) was not taken into account.

[d] Hydrodynamic diameter ($D_h$) and size distributions were measured by dynamic light scattering (DLS) in H$_2$O. See ESI for experimental details.

[e] Glass transition temperature: determined by the second heating curve of DSC.

This is due to low re-initiation efficiency of a polyacrylamide macroCTA towards acrylate monomer considering the large amount of the acrylate monomer in the second block.[63] The high molecular weight shoulder evident in the SEC trace of **AB$_2$** copolymer (Figure S6) is likely associated to the copolymerization of macromonomer formed by the propagating radical undergoing backbiting β-scission during the radical polymerization of acrylates,[64, 65] which will not affect the following cross-linking reaction.

As shown in Scheme 1d, the intramolecular cross-linking of the linear polymer chains was realized by the reaction of the pendent diol groups along the polymer backbone with a cross-linker. In order to reduce the competing intermolecular cross linking, the reaction is usually carried out at high dilutions (~10$^{-5}$ – 10$^{-6}$ mol·L$^{-1}$).[31] However, even in dilute conditions, intermolecular cross linking is still unavoidable.[66] In order to solve this problem, Hawker *et al.* developed a continuous addition method (by adding the solution of one reactant dropwise to the solution of the other reactant).[31] In this work, the synthesis of the tadpole-like SCNPs was carried out applying the continuous addition method. For the presented system, the solution of cross-linker Benzene-1,4-diboronic acid (DBA, 0.5 equivalent per diol group) was added dropwise (*i.e.* 15 minutes for **AB$_1$**, 30 minutes for **AB$_2$**, see the Supporting Information for a detailed procedure) into a premade basic aqueous solution (pH = 10) of the linear polymer precursor to fold the

second block. In order to investigate whether the single chain folding was successful, SEC, dynamic light scattering (DLS), and differential scanning calorimetry (DSC) analysis were performed.

SEC is an ideal technique to monitor any changes in the hydrodynamic volume of a polymer chain allowing to distinguish between linear precursors, SCNP and intermolecular cross linked species.[67-70] Comparing the SEC chromatograms of the obtained materials with their parent linear copolymers, a shift towards lower molar mass (*i.e.* smaller hydrodynamic volume, Figure 1) was observed for both cross-linking reactions, suggesting the successful formation of single chain polymeric nanoparticles **AB$_1^{SCNP}$** and **AB$_2^{SCNP}$**. These results are consistent with previous literature about the intramolecular cross linking of a single polymer chain.[33, 43, 66, 71-74] The compaction parameter $<G>$ calculated according to the method of Lutz *et al.*,[67] by comparison of the maximum peak values of the linear precursor and the compacted polymer chains, was obtained to be 0.90 and 0.86 for **AB$_1^{SCNP}$** and **AB$_2^{SCNP}$**, respectively (Table 1). These values closely match those of tadpole-like (P-shaped) macromolecules reported by Lutz *et al.*.[67] The relatively smaller $<G>$ value of **AB$_2^{SCNP}$** is likely due to the more significant extent of folding of **AB$_2$** given the relative more amount of cross-linkable units.
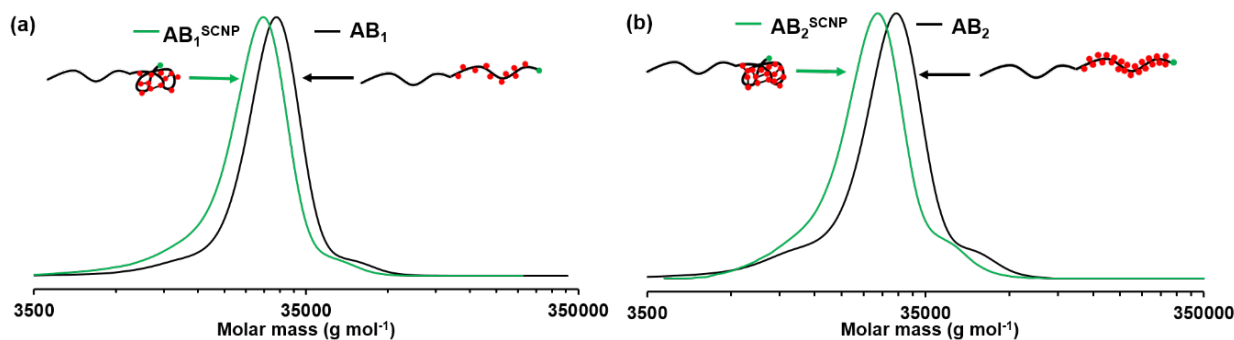


**Figure 1.** SEC chromatograms (RI traces) obtained in DMF for: (a) **AB$_1$** and **AB$_1^{SCNP}$**; (b) **AB$_2$** and **AB$_2^{SCNP}$**.
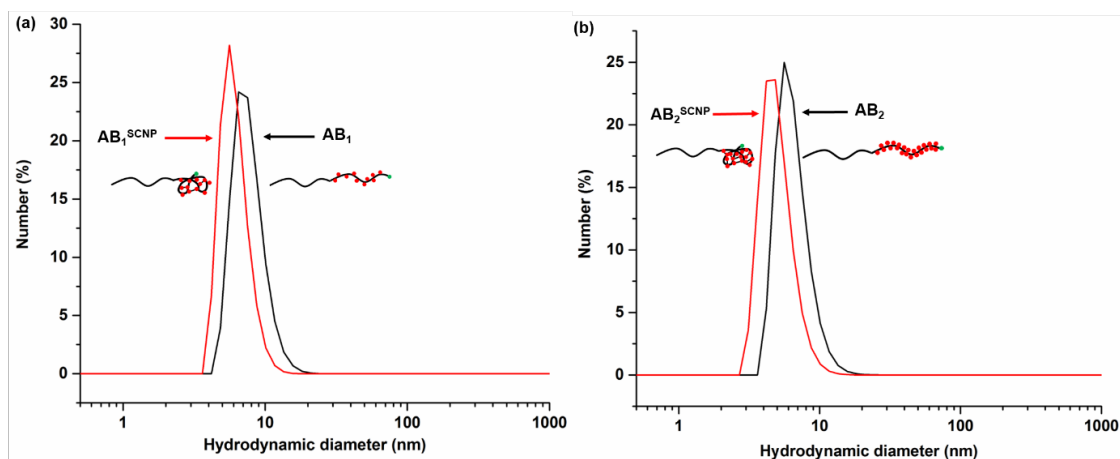
**Figure 2.** Hydrodynamic size distributions obtained by DLS in H$_2$O for (a) **AB$_1$** and **AB$_1$$^{SCNP}$** (pH = 10.02); (b) **AB$_2$** and **AB$_2$$^{SCNP}$** (pH = 10.20).

DLS measurements revealed a characteristic decrease in hydrodynamic diameter ($D_h$) of **AB$_1$$^{SCNP}$** and **AB$_2$$^{SCNP}$** compared to the corresponding linear precursor, which further indicates the intramolecular collapse and the formation of SCNPs (Figure 2). The average hydrodynamic diameter decreased from 7.7 nm for **AB$_1$** to 6.1 nm for **AB$_1$$^{SCNP}$** and from 6.5 nm for **AB$_2$** to 5.0 nm for **AB$_2$$^{SCNP}$** (Table 1).

DSC analysis was also conducted to demonstrate the successful formation of SCNPs. Compared to the linear polymer, the chain mobility of SCNPs will decrease, resulting in an increased glass transition temperature ($T_g$) value.[31, 75-77] The $T_g$ value of the **AB$_1$$^{SCNP}$** increased significantly to 172.4 °C from the initial value of 147.9 °C for linear polymer **AB$_1$** (Table 1, Figure S7, the value at around 90 °C was identified as measurement artefact, see Figure S8 and the ESI for the detailed explanation). On the other hand, the linear copolymer **AB$_2$** contains a larger fraction of GLA in the second block (**B$_2$**) which leads to a broader glass transition process and a decreased $T_g$ (95.8 °C, Table 1, Figure S9) compared to **AB$_1$** (147.9 °C). The disappearance of the $T_g$ value at 95.8 °C and the characteristic glass transition process with the $T_g$ value of 172.6 °C (Figure S9) indicate the successful compaction of **AB$_2$** leading to the formation of **AB$_2$$^{SCNP}$**. The more dramatic change of $T_g$ for **AB$_2$$^{SCNP}$** should be caused by the higher degree of compaction which is consistent with the SEC results.

Due to the wide pH ranges present in biological and physiological systems the application of pH-responsive polymeric nanoparticles for controlled encapsulation and release is of great interest.[78] The self-assembly behaviour of the tadpole-like SCNPs was investigated by varying the environmental pH. At high pH, the cross-linker exists as hydrophilic anionic boronate esters (Scheme 1a and 1d),[52, 79] therefore both segments of the diblock copolymers are hydrophilic. As the pH is lowered to neutral (pH ≈ 7.5), the majority of the cross-linker will become neutral, hydrophobic boronic esters, causing the tadpole-like SCNPs to be amphiphilic. This in turn will result in a phase segregation of the hydrophobic cross linked "head" block to form the core of a micellar assembly whereas the hydrophilic "tail" segment of NAM constitutes the shell. If the pH is further lowered to acidic condition, the boronic esters will be hydrolysed to yield free boronic acids and diols (Scheme 1b).[79]

The self-assembly behaviour of tadpole-like SCNPs adapting the pH changes was monitored by DLS analysis. When the pH of the aqueous solution of the **AB$_1$$^{SCNP}$** was gradually lowered from basic

(pH = 10.02) to acidic (pH = 2.36), the particles displayed similar sizes across the whole range and no self-assembly was observed (Table S1 and Figure S10). On the other hand, when the pH of the aqueous solution of the **AB$_2$$^{SCNP}$** was lowered from basic to neutral, multimolecular aggregates were observed which indicated the occurrence of self-assembly. The hydrodynamic diameters of **AB$_2$$^{SCNP}$** increased from 5.0 nm (at pH 10.20) to 111 nm and 245 nm at pH 8.00 and 7.60, respectively (Table S2, Figures 3 and S11), revealing the aggregate size could vary depending on the pH. Upon further lowering the pH to acidic, DLS displayed the dissociation of the aggregates and hydrolysis of the boronic esters leading to the formation of polymers with slightly bigger sizes than **AB$_2$$^{SCNP}$** at basic condition (Table S2, Figure S11). This phenomena is consistent with the assumption that assembled micellar structures were formed, composed of a hydrophilic polyNAM shell and a hydrophobic core, the size of which gradually increases when the pH was decreased as the anionic/hydrophilic boronate esters groups were converted to neutral/hydrophobic boronic esters groups. Once the pH-value reached to a critical level, the hydrolysis of boronic esters started occurring and led the dissociation of the micelles. It is noteworthy that at acidic condition (pH ≈ 2), **AB$_1$$^{SCNP}$** still displays a similar size as basic condition, whereas **AB$_2$$^{SCNP}$** shows an increased size value. $^1$H NMR and SEC studies were utilized to investigate the transition further.
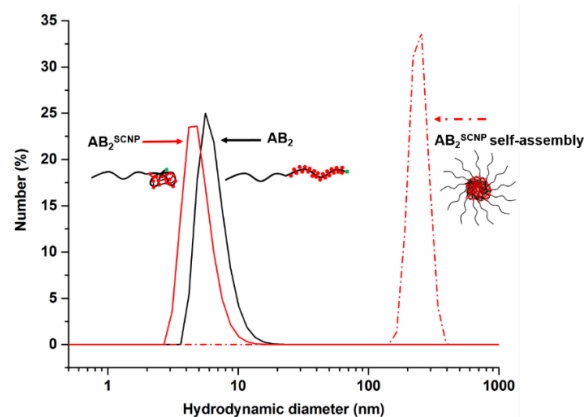


**Figure 3.** Hydrodynamic size distributions obtained by DLS in H$_2$O for: **AB$_2$**, **AB$_2$$^{SCNP}$** at pH = 10.20, and **AB$_2$$^{SCNP}$** self-assembly at pH = 7.60.
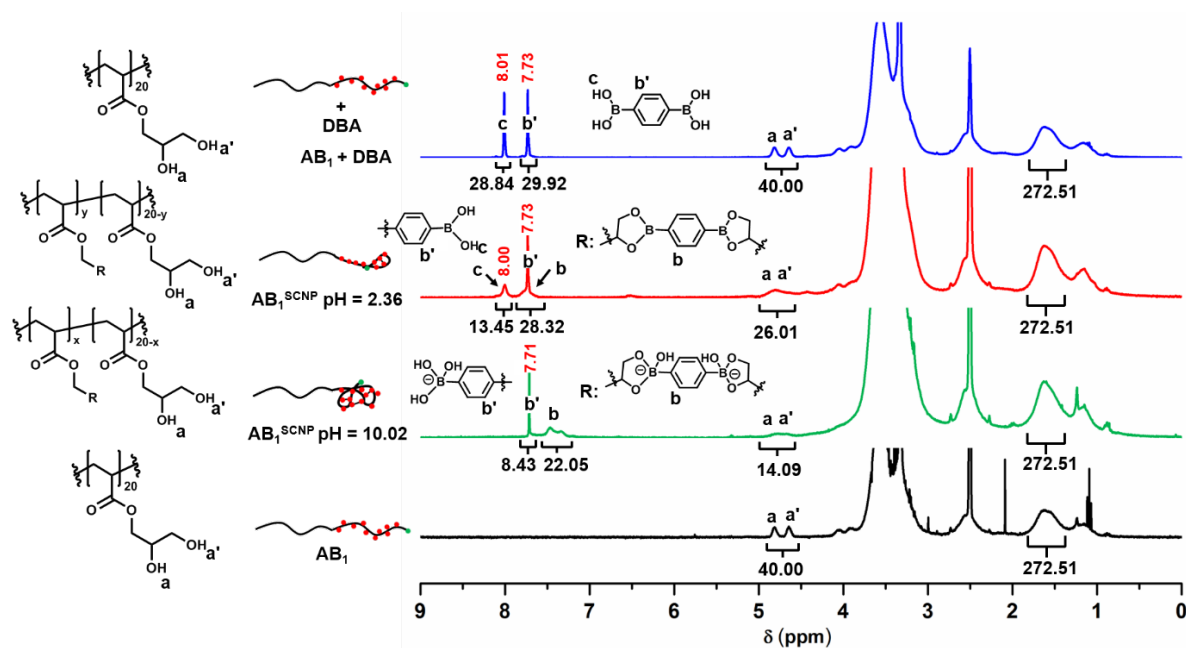
**Figure 4.** $^1$H NMR spectra (300MHz, DMSO-$d_6$) of: (from bottom to top) linear copolymer **AB$_1$**, folded copolymer **AB$_1^{SCNP}$** at pH = 10.02, folded copolymer **AB$_1^{SCNP}$** at pH = 2.36, and linear copolymer **AB$_1$** mixed with free DBA cross-linker in DMSO-$d_6$.

In order to be able to monitor the hydrolysis of boronic esters, DMSO-$d_6$ was used to observe the appearance of O*H* groups of GLA unit. $^1$H NMR spectroscopy investigation of **AB$_1$** and **AB$_1^{SCNP}$** in DMSO-$d_6$ was examined first (Figure 4, the integral of the peaks between $\delta$ = 1.90 and 1.30 ppm was used as internal reference, see the methods part in the ESI for how to integrate these peaks). The spectrum of **AB$_1^{SCNP}$** at pH 10.02 revealed the appearance of signals associated with cross linked DBA (peak b; for a comparison with free DBA mixed with free linear polymer **AB$_1$**, see the top spectrum in Figure 4; for a comparison with free DBA and free DBA at pH ≈ 10, see Figures S12 and S13, respectively). The spectrum displayed the signals of unreacted diol groups (peaks a and a') which is probably due to the high steric hindrance after the folding of the polymer.[70, 71] The $^1$H NMR spectroscopy of **AB$_1^{SCNP}$** in acidic condition (pH = 2.36) revealed that the integral of the signals associated with the free diol (peaks a and a') increased to 26.01 from 14.09 (for pH = 10.02), indicating 46 % [(26.01-14.09) ÷ (40.00-14.09) = 46%, see the ESI for a detailed explanation] hydrolysis of the total number of boronic esters. Similarly the integration of aromatic protons (peaks b + b') and O*H* groups (peak c) corresponding to DBA cross-linker also demonstrates equivalent value for hydrolysis. This equates to a value between 100% and 53% of the cross-linker still being attached to the polymer backbone depending on the number of DBA existing as a mono-boronic ester (100%, meaning all the DBA units were attached to the polymer backbone by one side) and di-boronic ester [53%, in this case all the O*H* groups (peak c) corresponding to DBA cross-linker belong to free DBA units, therefore the amount of the cross-linker still being attached to the polymer backbone is 28.32 − 13.45 = 14.87. The percentage of the attached DBA is therefore calculated to be 14.87 ÷ 28.32 = 53%] respectively. It is noteworthy the signals of aromatic protons (peak b) corresponding to the DBA cross-linker attached to the polymer chain shifted downfield at lower pH. This is consistent with the fact that boronate esters are negatively charged at high pH causing a rich electron environment (low chemical shift) around the aromatic ring and poor electron environment (high chemical shift) when uncharged at low pH.

We found **AB$_2^{SCNP}$** to be insoluble in the NMR solvent we used for this investigation, due to the high density of anionic boronate ester formed (see Figure S14 for DBA at pH ≈ 10 in DMSO-$d_6$). However, the $^1$H NMR spectrum of **AB$_2^{SCNP}$** in acidic condition (pH = 2.50, Figure S15) also displays similar profile to that of **AB$_1^{SCNP}$**, revealing between 84% and 42% (see the ESI for the detailed method of calculation) of DBA cross-linker still attached to the polymer backbone.

SEC analysis of the **AB$_1^{SCNP}$** at acidic condition (pH = 2.36) displays slightly smaller hydrodynamic volume compared to linear precursor **AB$_1$** (<$G$> = 0.96, Figure S16) but higher hydrodynamic volume than **AB$_1^{SCNP}$** at pH = 10.02 which is consistent with the hydrolysis of the boronic esters. This minor shift is likely to be associated with the low amount of residual intramolecular cross-linking. It is noteworthy that SEC analysis of self-assembled **AB$_2^{SCNP}$** at around neutral condition (pH = 7.60) demonstrates the retention of tadpole-like SCNPs structure with no apparent intermolecular exchange of the DBA cross-linker (Figure S17). Despite the close proximity of the hydrophobic "heads" in solution and dynamic nature of the boronic ester, intermolecular exchange of the DBA cross-linker was not apparent, otherwise a higher molar mass shoulder will be observed in the SEC trace. Moreover, a smaller compaction parameter (<$G$> = 0.78, Table S3) compared to **AB$_2^{SCNP}$** at pH = 10.20 (<$G$> = 0.86) was observed. We suspect the anionic boronate esters are more solvated due to the solvent screening the charge, hence neutralising the charge reduces the swelling. The SEC trace of the **AB$_2^{SCNP}$** in acidic conditions (pH = 2.50) shows a shift towards higher molar mass compared to **AB$_2^{SCNP}$** at pH =7.60, suggesting the hydrolysis of the boronic esters (Figure S17). However, compared to the linear precursor, it still displays lower molar mass distribution indicating intramolecular cross-linking (<$G$> = 0.88, Table S3). These results are consistent with the $^1$H NMR analysis.
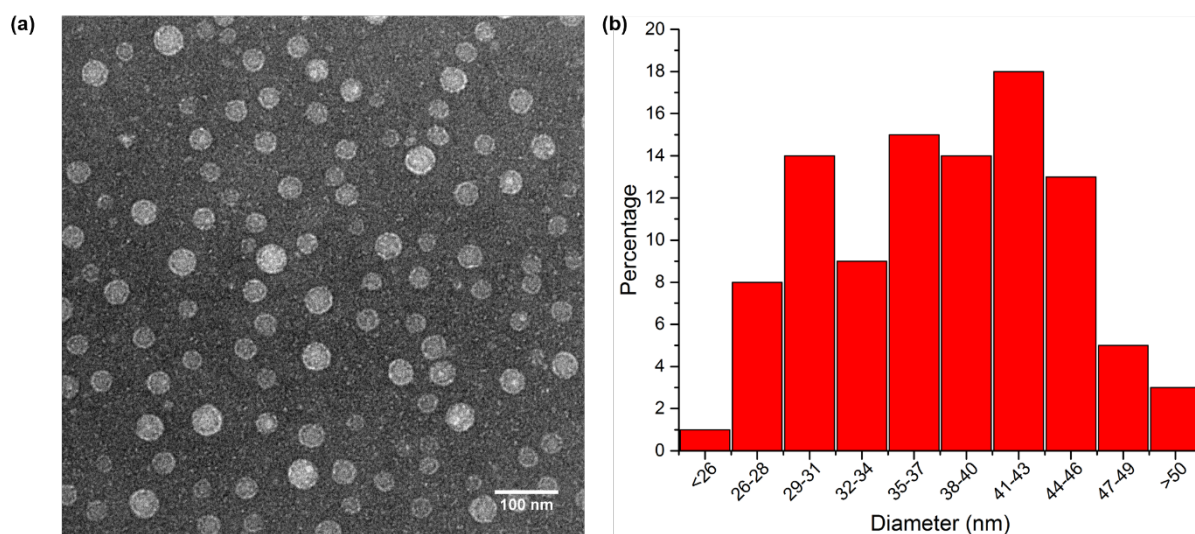
**Figure 5.** Representative image of nanoparticles formed by the self-assembly of $AB_2^{SCNP}$ obtained by TEM (a) and size distributions of nanoparticles analyzed from TEM results (b).



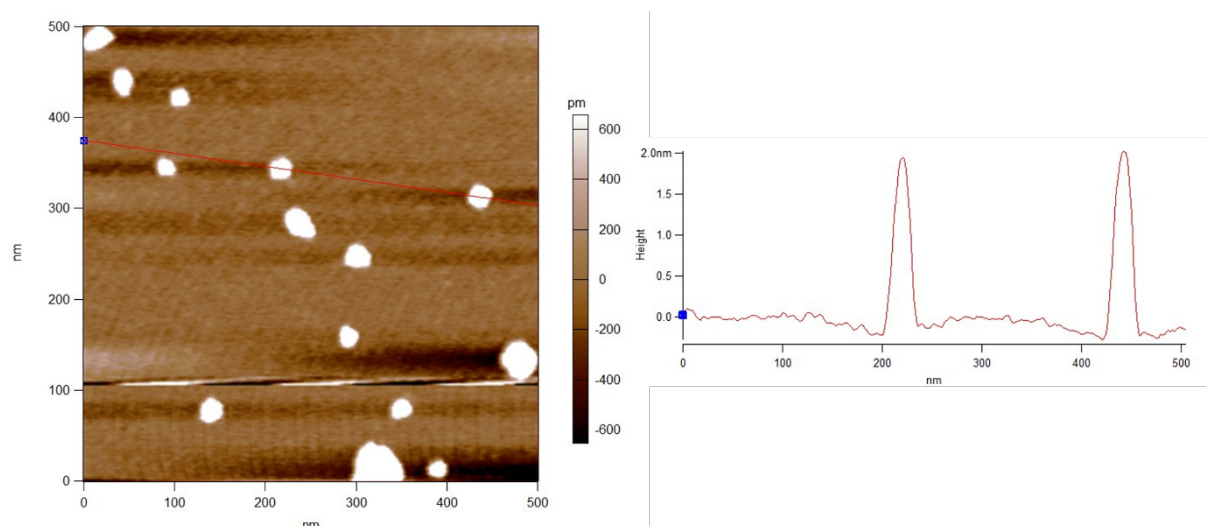**Figure 6.** Representative AFM topography image of nanoparticles formed by the self-assembly of $AB_2^{SCNP}$. The red line in the topography image shows the analyzed particles.

The more pronounced compaction displayed by $AB_2^{SCNP}$ compared to $AB_1^{SCNP}$ in acidic condition is likely due to the increased amount of cross-linker in $AB_2^{SCNP}$ which caused the de-crosslinking to be less efficient.

It is interesting to notice that while DMF-SEC of $AB_1^{SCNP}$ in acidic condition (pH = 2.36) only shows a minor shift towards lower molar mass compared to $AB_1$ (Figure S16) but DLS still displays similar size to $AB_1^{SCNP}$ in basic condition (Table S1, Figure S10); whereas $AB_2^{SCNP}$ in acidic condition (pH = 2.50) reveals a relatively big shift toward lower molar mass compared to $AB_2$ by DMF-SEC (Figure S17) but displays bigger size distribution than $AB_2^{SCNP}$ in basic condition in DLS (Table S2, Figure S11). This is probably due to the hydrophobicity of the remaining DBA cross-linker attached to $AB_1^{SCNP}$ in acidic condition causing the chains to collapse in $H_2O$ leading to the smaller size as reflected by DLS. On the other hand, considering there are still relative high amount of DBA cross-linkers in $AB_2^{SCNP}$ in acidic condition as illustrated by DMF-SEC (Figure S17), these hydrophobic DBA cross-linkers will still cause the aggregation

of $AB_2^{SCNP}$ to a certain extent which caused bigger sizes than $AB_2^{SCNP}$ in basic condition but are insufficient for self-assembly into bigger particles. Therefore, it is reasonable to assume $AB_2^{SCNP}$ in acidic condition in $H_2O$ is composed of small self-assembled aggregates consisting of amphiphilic tadpole-like SCNPs with a low degree compaction. The reason why $AB_1^{SCNP}$ did not self-assemble into micellar structures was hypothesized due to the low amount of the boronate ester compared to $AB_2^{SCNP}$ as a result of the low diol content of $AB_1$, and therefore insufficient hydrophobicity to promote self-assembly.

Transmission electron microscopy (TEM) and atomic force microscopy (AFM) imaging were employed to further explore the morphology of the nanoparticles formed by self-assembly of $AB_2^{SCNP}$ at pH 7.60 in aqueous solution. Spherical nano-objects with diameter sizes of around 38 (± 6.6) nm were visualized by TEM (Figures 5 and S18). AFM also revealed nanoparticles with similar diameter values to TEM (Figures 6, S19 and S20, samples used for TEM and AFM were diluted by 10 times after self-assembly of

$AB_2^{SCNP}$ at pH = 7.60). The relatively small size compared to the values obtained by DLS analysis could be due to a shrinking of the samples in dry state, whereas water-swollen structures were observed in aqueous solution using DLS.
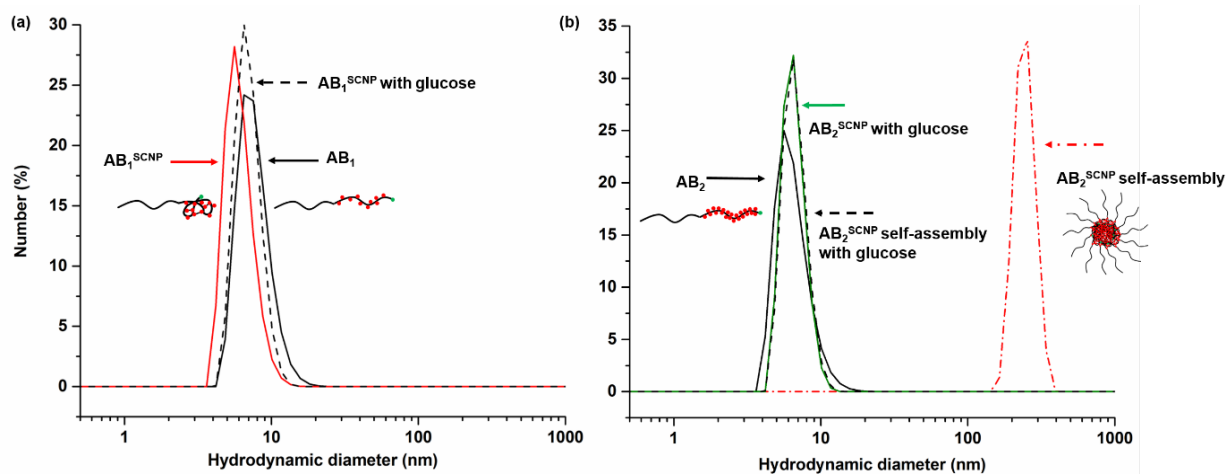


**Figure 7.** Hydrodynamic size distributions obtained by DLS in $H_2O$ for: (a) $AB_1^{SCNP}$ at pH = 10.02, $AB_1^{SCNP}$ with addition of glucose at pH = 10.02, and linear copolymer $AB_1$; (b) linear copolymer $AB_2$, $AB_2^{SCNP}$ with addition of glucose at pH = 10.20, $AB_2^{SCNP}$ self-assembly with addition of glucose at pH = 7.60, and $AB_2^{SCNP}$ self-assembly at pH = 7.60.

In addition to the pH responsive nature, the diol responsiveness of the tadpole-like SCNPs and the self-assembled micelles was also investigated in order to exploit the potential applications in sensors for sugars.[80] Due to the reversible nature of the dynamic covalent bond of the cyclic boronate/boronic esters formed by the boronic acid groups with 1,2- and 1,3-diols,[52, 80] the free diol containing molecules will competitively react with boronic ester *via* transesterification. Upon the addition of glucose to the aqueous solution of the $AB_1^{SCNP}$ and $AB_2^{SCNP}$ at basic condition, decross-linking of the SCNPs was triggered leading to polymers with similar sizes to the respective linear precursor as detected by DLS (Figure 7). SEC analysis of the SCNPs samples treated with sugar also revealed similar molar mass distributions to the corresponding linear copolymers (Figures S21 and S22). Addition of glucose to the solution of micelles formed by self-assembly of $AB_2^{SCNP}$ at pH 7.60 caused the disruption of self-assembled structure and led the formation of unimers as displayed by DLS showing similar hydrodynamic diameter to the linear $AB_2$ (Figure 7b). In addition to the DLS results, dissociation was also illustrated by SEC (Figure S22) analysis which shows similar molar mass distribution to $AB_2$ precursor for the disassembled sample.

## Conclusions

In summary, tadpole-like SCNPs were synthesised using a pH responsive DBA cross-linker and suitable linear polymer precursors, which exhibited self-assembly due to the hydrophobic nature of cross-linker past its isoelectric point. The assembled SCNPs displayed spherical morphology as characterised by TEM and AFM. The intramolecular folding of individual SCNPs was intact and no chain entanglement occurred after self-assembly according to the SEC. We found that the volume fraction of cross-linkable GLA in the second block to play a crucial role in the self-assembly of the SCNP, as sufficient hydrophobicity is required to promote the "head" group to drive self-assembly. The dissociation of assemblies can be triggered by varying the environmental pH or exposing to an external stimuli as demonstrated by addition of glucose. The use of boronic acid containing polymers for pH dependent self-assembly

has been demonstrated elsewhere, however, forming a SCNP with boronic acid cross-linker and taking advantage of its stimuli-responsive properties to drive self-assembly, has not been reported. The present study demonstrates the ability of synthetic polymers to mimic folding of natural polypeptide chains and assembly into a higher-order structure found in natural multiprotein complexes, which also display a stimuli responsive character. We hope this study will encourage more research on this active area and provide more perspective for building more complexed biomimetic self-assembled structures with the potential application in healthcare.

## Acknowledgements

## Notes and references

1.      C. B. Anfinsen, *Science*, 1973, **181**, 223-230.
2.      C. M. Dobson, *Nature*, 2003, **426**, 884-890.
3.      C. S. Mahon and D. A. Fulton, *Nat. Chem.*, 2014, **6**, 665-672.
4.      M. A. C. Stuart, W. T. S. Huck, J. Genzer, M. Muller, C. Ober, M. Stamm, G. B. Sukhorukov, I. Szleifer, V. V. Tsukruk, M. Urban, F. Winnik, S. Zauscher, I. Luzinov and S. Minko, *Nat Mater*, 2010, **9**, 101-113.

5.    A. M. Hanlon, C. K. Lyon and E. B. Berda, *Macromolecules*, 2016, **49**, 2-14.
6.    C. K. Lyon, A. Prasher, A. M. Hanlon, B. T. Tuten, C. A. Tooley, P. G. Frank and E. B. Berda, *Polym. Chem.*, 2015, **6**, 181-197.
7.    M. Ouchi, N. Badi, J. F. Lutz and M. Sawamoto, *Nat. Chem.*, 2011, **3**, 917-924.
8.    O. Altintas and C. Barner-Kowollik, *Macromol. Rapid Commun.*, 2016, **37**, 29-46.
9.    O. Altintas and C. Barner-Kowollik, *Macromol. Rapid Commun.*, 2012, **33**, 958-971.
10.   M. Gonzalez-Burgos, A. Latorre-Sanchez and J. A. Pomposo, *Chem. Soc. Rev.*, 2015, **44**, 6122-6142.
11.   J. A. Pomposo, *Polym. Int.*, 2014, **63**, 589-592.
12.   A. Sanchez-Sanchez, I. Perez-Baena and J. A. Pomposo, *Molecules*, 2013, **18**, 3339-3355.
13.   S. Mavila, O. Eivgi, I. Berkovich and N. G. Lemcoff, *Chem. Rev.*, 2016, **116**, 878-961.
14.   M. Huo, N. Wang, T. Fang, M. Sun, Y. Wei and J. Yuan, *Polymer*, 2015, **66**, A11-A21.
15.   J. Zhang, G. Gody, M. Hartlieb, S. Catrouillet, J. Moffat and S. Perrier, *Macromolecules*, 2016, **49**, 8933-8942.
16.   N. Hosono, A. M. Kushner, J. Chung, A. R. A. Palmans, Z. Guan and E. W. Meijer, *J. Am. Chem. Soc.*, 2015, **137**, 6880-6888.
17.   T. Mes, R. van der Weegen, A. R. Palmans and E. W. Meijer, *Angew. Chem. Int. Ed. Engl.*, 2011, **50**, 5085-5089.
18.   N. Hosono, A. R. A. Palmans and E. W. Meijer, *Chem. Commun.*, 2014, **50**, 7990-7993.
19.   O. Altintas, P. Krolla-Sidenstein, H. Gliemann and C. Barner-Kowollik, *Macromolecules*, 2014, **47**, 5877-5888.
20.   O. Altintas, E. Lejeune, P. Gerstel and C. Barner-Kowollik, *Polym. Chem.*, 2012, **3**, 640-651.
21.   E. H. H. Wong, S. J. Lam, E. Nam and G. G. Qiao, *ACS Macro Letters*, 2014, **3**, 524-528.
22.   J. B. Beck, K. L. Killops, T. Kang, K. Sivanandan, A. Bayles, M. E. Mackay, K. L. Wooley and C. J. Hawker, *Macromolecules*, 2009, **42**, 5629-5635.
23.   O. Shishkan, M. Zamfir, M. A. Gauthier, H. G. Borner and J.-F. Lutz, *Chem. Commun.*, 2014, **50**, 1570-1572.
24.   O. Altintas, J. Willenbacher, K. N. R. Wuest, K. K. Oehlenschlaeger, P. Krolla-Sidenstein, H. Gliemann and C. Barner-Kowollik, *Macromolecules*, 2013, **46**, 8092-8101.
25.   A. M. Hanlon, I. Martin, E. R. Bright, J. Chouinard, K. J. Rodriguez, G. E. Patenotte and E. B. Berda, *Polym. Chem.*, 2017, DOI: 10.1039/C7PY00320J.
26.   R. Lambert, A.-L. Wirotius and D. Taton, *ACS Macro Letters*, 2017, DOI: 10.1021/acsmacrolett.7b00161, 489-494.
27.   T.-K. Nguyen, S. J. Lam, K. K. K. Ho, N. Kumar, G. G. Qiao, S. Egan, C. Boyer and E. H. H. Wong, *ACS Infectious Diseases*, 2017, **3**, 237-248.
28.   T. S. Fischer, D. Schulze-Sünninghausen, B. Luy, O. Altintas and C. Barner-Kowollik, *Angew. Chem. Int. Ed.*, 2016, **55**, 11276-11280.
29.   N. D. Knöfel, H. Rothfuss, J. Willenbacher, C. Barner-Kowollik and P. W. Roesky, *Angew. Chem. Int. Ed.*, 2017, **56**, 4950-4954.
30.   M. Aiertza, I. Odriozola, G. Cabañero, H.-J. Grande and I. Loinaz, *Cell. Mol. Life Sci.*, 2012, **69**, 337-346.
31.   E. Harth, B. V. Horn, V. Y. Lee, D. S. Germack, C. P. Gonzales, R. D. Miller and C. J. Hawker, *J. Am. Chem. Soc.*, 2002, **124**, 8653-8660.
32.   E. B. Berda, E. J. Foster and E. W. Meijer, *Macromolecules*, 2010, **43**, 1430-1437.
33.   B. S. Murray and D. A. Fulton, *Macromolecules*, 2011, **44**, 7242-7252.
34.   N. Hosono, M. A. J. Gillissen, Y. Li, S. S. Sheiko, A. R. A. Palmans and E. W. Meijer, *J. Am. Chem. Soc.*, 2013, **135**, 501-510.
35.   N. J. W. Penfold, J. R. Lovett, P. Verstraete, J. Smets and S. P. Armes, *Polym. Chem.*, 2017, **8**, 272-282.
36.   I. Cobo, M. Li, B. S. Sumerlin and S. Perrier, *Nat Mater*, 2015, **14**, 143-159.
37.   B. Surnar and M. Jayakannan, *Biomacromolecules*, 2013, **14**, 4377-4387.
38.   J. Du, L. Fan and Q. Liu, *Macromolecules*, 2012, **45**, 8275-8283.
39.   X. Sun and T. D. James, *Chem. Rev.*, 2015, **115**, 8001-8037.
40.   M. A. J. Gillissen, I. K. Voets, E. W. Meijer and A. R. A. Palmans, *Polym. Chem.*, 2012, **3**, 3166-3174.
41.   S. J. Rowan, S. J. Cantrill, G. R. L. Cousins, J. K. M. Sanders and J. F. Stoddart, *Angew. Chem. Int. Ed.*, 2002, **41**, 898-952.
42.   D. E. Whitaker, C. S. Mahon and D. A. Fulton, *Angew. Chem. Int. Ed.*, 2013, **52**, 956-959.
43.   A. Sanchez-Sanchez, D. A. Fulton and J. A. Pomposo, *Chem. Commun.*, 2014, **50**, 1871-1874.
44.   A. Sanchez-Sanchez and J. A. Pomposo, *Particle & Particle Systems Characterization*, 2014, **31**, 11-23.
45.   W. L. A. Brooks and B. S. Sumerlin, *Chem. Rev.*, 2016, **116**, 1375-1397.
46.   J. Ren, Y. Zhang, J. Zhang, H. Gao, G. Liu, R. Ma, Y. An, D. Kong and L. Shi, *Biomacromolecules*, 2013, **14**, 3434-3443.
47.   F. Coumes, P. Woisel and D. Fournier, *Macromolecules*, 2016, **49**, 8925-8932.
48.   J. N. Cambre and B. S. Sumerlin, *Polymer*, 2011, **52**, 4631-4643.
49.   C. C. Deng, W. L. A. Brooks, K. A. Abboud and B. S. Sumerlin, *ACS Macro Letters*, 2015, **4**, 220-224.
50.   P. De, S. R. Gondi, D. Roy and B. S. Sumerlin, *Macromolecules*, 2009, **42**, 5614-5621.
51.   A. P. Bapat, D. Roy, J. G. Ray, D. A. Savin and B. S. Sumerlin, *J. Am. Chem. Soc.*, 2011, **133**, 19832-19838.
52.   D. Roy, J. N. Cambre and B. S. Sumerlin, *Chem. Commun.*, 2009, DOI: 10.1039/B900374F, 2106-2108.
53.   J. O. Edwards, G. C. Morrison, V. F. Ross and J. W. Schultz, *J. Am. Chem. Soc.*, 1955, **77**, 266-268.
54.   J. P. Lorand and J. O. Edwards, *J. Org. Chem.*, 1959, **24**, 769-774.
55.   A. Blanazs, S. P. Armes and A. J. Ryan, *Macromol. Rapid Commun.*, 2009, **30**, 267-277.
56.   Y. Mai and A. Eisenberg, *Chem. Soc. Rev.*, 2012, **41**, 5969-5985.
57.   U. Haldar, M. Nandi, B. Ruidas and P. De, *Eur. Polym. J.*, 2015, **67**, 274-283.
58.   F. Zhou, M. Xie and D. Chen, *Macromolecules*, 2014, **47**, 365-372.
59.   J. Wen, L. Yuan, Y. Yang, L. Liu and H. Zhao, *ACS Macro Letters*, 2013, **2**, 100-106.
60.   B. Smagowska and M. Pawlaczyk-Łuszczyńska, *Int. J. Occup. Saf. Ergonomics*, 2013, **19**, 195-202.

61. S. C. O. Sousa, C. G. L. Junior, F. P. L. Silva, N. G. Andrade, T. P. Barbosa and M. L. A. A. Vasconcellos, *J. Braz. Chem. Soc.*, 2011, **22**, 1634-1643.
62. G. Gody, T. Maschmeyer, P. B. Zetterlund and S. Perrier, *Macromolecules*, 2014, **47**, 3451-3460.
63. L. Martin, G. Gody and S. Perrier, *Polym. Chem.*, 2015, **6**, 4875-4886.
64. A. Postma, T. P. Davis, G. Li, G. Moad and M. S. O'Shea, *Macromolecules*, 2006, **39**, 5307-5318.
65. G. Moad and C. Barner-Kowollik, in *Handbook of RAFT Polymerization*, Wiley-VCH Verlag GmbH & Co. KGaA, 2008, DOI: 10.1002/9783527622757.ch3, pp. 51-104.
66. R. K. Roy and J. F. Lutz, *J. Am. Chem. Soc.*, 2014, **136**, 12888-12891.
67. B. V. Schmidt, N. Fechler, J. Falkenhagen and J. F. Lutz, *Nat. Chem.*, 2011, **3**, 234-238.
68. J. A. Pomposo, I. Perez-Baena, L. Buruaga, A. Alegría, A. J. Moreno and J. Colmenero, *Macromolecules*, 2011, **44**, 8644-8649.
69. E. J. Foster, E. B. Berda and E. W. Meijer, *J. Am. Chem. Soc.*, 2009, **131**, 6964-6966.
70. B. T. Tuten, D. Chao, C. K. Lyon and E. B. Berda, *Polym. Chem.*, 2012, **3**, 3068-3071.
71. J. B. Beck, K. L. Killops, T. Kang, K. Sivanandan, A. Bayles, M. E. Mackay, K. L. Wooley and C. J. Hawker, *Macromolecules*, 2009, **42**, 5629-5635.
72. C. Heiler, J. T. Offenloch, E. Blasco and C. Barner-Kowollik, *ACS Macro Letters*, 2017, **6**, 56-61.
73. A. M. Hanlon, R. Chen, K. J. Rodriguez, C. Willis, J. G. Dickinson, M. Cashman and E. B. Berda, *Macromolecules*, 2017, **50**, 2996-3003.
74. J. A. Pomposo, J. Rubio-Cervilla, A. J. Moreno, F. Lo Verso, P. Bacova, A. Arbe and J. Colmenero, *Macromolecules*, 2017, **50**, 1732-1739.
75. D. Mecerreyes, V. Lee, C. J. Hawker, J. L. Hedrick, A. Wursch, W. Volksen, T. Magbitang, E. Huang and R. D. Miller, *Adv. Mater.*, 2001, **13**, 204-208.
76. A. E. Cherian, F. C. Sun, S. S. Sheiko and G. W. Coates, *J. Am. Chem. Soc.*, 2007, **129**, 11350-11351.
77. C. Song, L. Li, L. Dai and S. Thayumanavan, *Polym. Chem.*, 2015, **6**, 4828-4834.
78. J. Du and R. K. O'Reilly, *Soft Matter*, 2009, **5**, 3544-3561.
79. D. Roy and B. S. Sumerlin, *ACS Macro Letters*, 2012, **1**, 529-532.
80. H. Fang, G. Kaur and B. Wang, *Journal of Fluorescence*, 2004, **14**, 481-489.

**Graphical Abstract**